University of Texas Rio Grande Valley

ScholarWorks @ UTRGV

Physics and Astronomy Faculty Publications and Presentations

College of Sciences

2014

Fluid dynamic modeling of nano-thermite reactions

Karen S. Martirosyan
The University of Texas Rio Grande Valley

Maxim Zyskin
Rutgers University - New Brunswick/Piscataway

Charles M. Jenkins
Eglin AFB

Yasuyuki Horie
Eglin AFB

Follow this and additional works at: https://scholarworks.utrgv.edu/pa_fac

Part of the Nanoscience and Nanotechnology Commons, and the Physics Commons

Recommended Citation

Fluid dynamic modeling of nano-thermite reactions

Karen S. Martirosyan,[1,a)] Maxim Zyskin,[2] Charles M. Jenkins,[3] and Yasuyuki (Yuki) Horie[3]

[1]*Department of Physics and Astronomy, University of Texas, Brownsville, 80 Fort Brown, Brownsville, Texas 78520, USA*
[2]*Rutgers University, 110 Frelinghusen Road, Piscataway, New Jersey 08854-8019, USA*
[3]*Air Force Research Laboratory, Munitions Directorate, 2306 Perimeter Road, Eglin AFB, Florida 32542, USA*

This paper presents a direct numerical method based on gas dynamic equations to predict pressure evolution during the discharge of nanoenergetic materials. The direct numerical method provides for modeling reflections of the shock waves from the reactor walls that generates pressure-time fluctuations. The results of gas pressure prediction are consistent with the experimental evidence and estimates based on the self-similar solution. Artificial viscosity provides sufficient smoothing of shock wave discontinuity for the numerical procedure. The direct numerical method is more computationally demanding and flexible than self-similar solution, in particular it allows study of a shock wave in its early stage of reaction and allows the investigation of "slower" reactions, which may produce weaker shock waves. Moreover, numerical results indicate that peak pressure is not very sensitive to initial density and reaction time, providing that all the material reacts well before the shock wave arrives at the end of the reactor. © *2014 AIP Publishing LLC*. [http://dx.doi.org/10.1063/1.4867936]

I. INTRODUCTION

Nanostructured highly exothermic reactive mixtures, referred to as Nanoenergetic Materials (NMs) or Metastable Intermolecular Composites (MICs), may release energy much faster than conventional energetic materials.[1–7] The size reduction of reactant powders from micro- to nano-size increases the reaction front propagation velocity in some systems by two to three orders of magnitude.[8] This is presumably due to the reduction of the diffusion distance between nanostructured grains of the intermixed reactants, and rapid oxidation time-scale for nano-sized metal particles.[9–14] Modeling of nanoenergetic materials based on thermite reactions was initiated recently[15] and was based on a self-similar solution. A self-similar solution has been shown to provide a relatively suitable match with experimental data,[16] when drag coefficients (or Zel'dovich-Raizer relation[17] for a wall impact) are used to account for disturbance created by a detector or a closed reactor wall. A self-similar solution is given by explicit analytical expressions, thus computations based on a self-similar solution are quick. Results produced by Ref. 15 suggest that a self-similar solution is well suitable to describe a pressure wave created by a very fast nanoenergetic reaction. However, the self-similar solution also has certain limitations: it does not account for a finite reaction time, which affects pressure wave fluctuations. It starts with a singularity and does not accurately describe early stages of the explosion and it also does not provide an accurate description of multiple reflections observed in our experiments.

In this paper, a direct numerical method for solving fluid dynamic equations was investigated. Our model assumes that solid nanoenergetic material undergoes a highly exothermic and high rate chemical reaction to a gaseous phase. Such reaction occurs with a defined rate, matched with experimental and modeling data reported in Ref. 11. We model numerically the fluid dynamics throughout the chemical reaction process and after the reaction's completion.

We assume that explosion occurs in the middle of a cylindrical reactor and that fluid motion is uniform in a circular cross-section of a cylindrical reactor, closed at both ends, as illustrated in Figure 1. Reactor volume is 0.342 l, length is 11.5 cm, and it is filled with air. Pressure is measured by the detectors placed near closed reactor walls, far away from the fuel region. In our computation, length of the fuel region is taken to be 3.3 mm.

A numerical solution may have a shock wave discontinuity, the location of which is not known in advance; thus numerical methods should be able to accommodate such discontinuous solutions.[18] We adopt the approach of Ref. 19, adding an artificial viscosity term Q, which is small when a solution is smooth but becomes significant when a solution is nearly discontinuous. The role of a viscosity term is to smear out discontinuities, enabling numerical solution to continue even after the shock wave develops; without an artificial viscosity regularization, numerical computation cannot be continued after the shock wave has been formed.

In our computational framework, we were able to trace the formation and dynamics of shock waves as well as the reflections from the reactor walls.

II. NUMERICAL SIMULATION: METHOD

In this report, we consider the direct numerical modeling of a one dimensional explosion which propagates along the axes of the cylindrical reactor.

For the model presented, let x be the Lagrangian coordinate, $X(x,t)$ the corresponding Eulerean coordinate, giving position of a fluid element which at $t = 0$ was at x (so $X(x,0) = x$.) Let $u(x,t) = \frac{\partial X}{\partial t}$ be the velocity, and $\nu(x,t) = \frac{1}{\rho_o(x)} \frac{\partial X}{\partial x}$ the specific volume; here, $\rho_o(x)$ is the initial

density. We will use a single fluid flow model. The gas dynamics equations in Lagrangian coordinates are represented as

$$\rho_0(x)\frac{\partial u}{\partial t} = -\frac{\partial}{\partial x}(P+Q),$$
$$\rho_0(x)\frac{\partial \nu}{\partial t} = \frac{\partial u}{\partial x}, \tag{1}$$
$$\frac{\partial \varepsilon}{\partial t} = -(P+Q)\frac{\partial \nu}{\partial t}.$$

Here ε is the internal energy per unit mass, which is a function of the other hydrodynamic quantities given by an equation of state for the fluid; and Q is the viscous term,

$$Q = -\frac{(c\Delta x)^2}{\nu}\frac{\partial u}{\partial x}\left|\frac{\partial u}{\partial x}\right|; \tag{2}$$

here Δx is the mesh size, and c is a dimensionless parameter. Without the viscous term, Eq. (1) is equivalent to the usual equations of gas dynamics, presented in Lagrangian coordinates. The gas dynamics equations are given by the Euler equation (or momentum conservation), and conservation of mass and energy.

The initial density is

$$\rho_0(x) = \rho_a(x) + \rho_e(x), \tag{3}$$

where $\rho_a(x)$ is the uniform air density ($\sim 1.2\,\frac{kg}{m^3}$), and $\rho_e(x)$ is the density of the nanoenergetic material, which we consider to be localized in a thin cross-section of a cylindrical reactor.

We assume that during the ignition stage nanoenergetic material undergoes a transition from a solid with the internal energy of $h_e \sim 2.12\,\frac{kJ}{g}$ corresponding to Al/Bi$_2$O$_3$ mixture), to an ideal gas with adiabatic index $\gamma = \frac{c_p}{c_v}$. To simplify the treatment, we assume that γ is the same for the vaporized nanoenergetic material and for the ambient gas. If $r(t)$ is a

switching function, describing the proportion of nanoenergetic material which has reacted up to time t,

$$r(t) = \begin{cases} 0, t \leq 0 \\ \frac{1}{2}\left(1+\tanh\left(\frac{\tau(t-\tau/2)}{2t(\tau-t)}\right)\right), 0 < t < \tau \\ 1, t \geq \tau, \end{cases} \tag{4}$$

where τ is reaction time. We note that $r(t)$ is nondecreasing and is smooth. Energy per unit mass, as a function of the Lagrangian coordinates x, t, has contributions from the chemical energy stored in the remaining nanomixture and from energy in the gaseous phase,

$$\varepsilon(x,t) = \frac{(1-r(t))\rho_e(x)}{\rho_0(x)}h_e + \frac{P(x,t)\eta(x,t)}{\gamma-1},$$
$$\eta(x,t) = \nu(x,t)\frac{\rho_0(x)}{\rho_a + r(t)\rho_e(x)}. \tag{5}$$

Here, $\frac{(1-r(t))\rho_e(x)}{\rho_0(x)}$ is the density proportion of the remaining energetic nanomaterial, and $\eta(x,t) = \nu(x,t)\frac{\rho_0(x)}{\rho_a + r(t)\rho_e(x)}$ is the the specific volume of the vaporized phase. Equation (5) implies that at time periods past the reaction time, $t \geq \tau$, all the stored chemical energy is released and all the material is in the gaseous state. Using the equation of state (5), the energy equation, the last equation in (1) becomes

$$\frac{1}{\gamma-1}\left(P\frac{\partial \eta}{\partial t} + \frac{\partial P}{\partial t}\eta\right) - \frac{dr(t)}{dt}\frac{\rho_e(x)}{\rho_0(x)}h_e = -(P+Q)\frac{\partial \nu}{\partial t}. \tag{6}$$

For the numerical simulation, we use a finite difference scheme

$$\frac{1}{2}\left((\rho_0)_{j+\frac{1}{2}} + (\rho_0)_{j-\frac{1}{2}}\right)\frac{u_j^{i+\frac{1}{2}} - u_j^{i-\frac{1}{2}}}{\Delta t} = -\frac{P_{j+\frac{1}{2}}^i + Q_{j+\frac{1}{2}}^{i-\frac{1}{2}} - P_{j-\frac{1}{2}}^i - Q_{j-\frac{1}{2}}^{i-\frac{1}{2}}}{\Delta x},$$

$$\frac{1}{2}\left((\rho_0)_{j+\frac{1}{2}} + (\rho_0)_{j-\frac{1}{2}}\right)\frac{\nu_{j+\frac{1}{2}}^{i+1} - \nu_{j+\frac{1}{2}}^i}{\Delta t} = \frac{u_{j+1}^{i+\frac{1}{2}} - u_j^{i+\frac{1}{2}}}{\Delta x},$$

$$Q_{j+\frac{1}{2}}^{i+\frac{1}{2}} = -\frac{2c^2}{\nu_{j+\frac{1}{2}}^i + \nu_{j+\frac{1}{2}}^{i+1}}\left(u_{j+1}^{i+\frac{1}{2}} - u_j^{i+\frac{1}{2}}\right)|u_{j+1}^{i+\frac{1}{2}} - u_j^{i+\frac{1}{2}}|, \tag{7}$$

$$\left(P_{j+\frac{1}{2}}^i + P_{j+\frac{1}{2}}^{i+1}\right)\left(\eta_{j+\frac{1}{2}}^{i+1} - \eta_{j+\frac{1}{2}}^i\right) + (\gamma-1)\left(P_{j+\frac{1}{2}}^i + P_{j+\frac{1}{2}}^{i+1} + 2Q_{j+\frac{1}{2}}^{i+\frac{1}{2}}\right)\left(\nu_{j+\frac{1}{2}}^{i+1} - \nu_{j+\frac{1}{2}}^i\right)$$

$$+\left(P_{j+\frac{1}{2}}^{i+1} - P_{j+\frac{1}{2}}^i\right)\left(\eta_{j+\frac{1}{2}}^i + \eta_{j+\frac{1}{2}}^{i+1}\right) = 2(\gamma-1)(r_{i+1} - r_i)\frac{(\rho_e)_{j+\frac{1}{2}}}{(\rho_0)_{j+\frac{1}{2}}}h_e,$$

where $P_{j+\frac{1}{2}}^i = P(x_{j+\frac{1}{2}}, t_i)$, etc., and η is the specific volume of the gaseous phase, $\eta_{j+\frac{1}{2}}^i = \nu_{j+\frac{1}{2}}^i\frac{(\rho_0)_{j+\frac{1}{2}}}{\rho_a + r^i(\rho_e)_{j+\frac{1}{2}}}$. The last equation in (7) is a discretization of the energy equation in the form of Eq. (6), which uses the equation of state given by (5). The finite difference scheme (7) is illustrated in Figure 2.

At times past the reaction time τ, $\eta \equiv \nu$, and the discrete scheme Eq. (7) becomes the same as the one considered in Ref. 19. Linear stability analysis in Ref. 19 indicates that the scheme is stable provided that the time step is sufficiently small,

$$\Delta t \leq \frac{\Delta x}{s}\frac{\gamma^{\frac{1}{2}}}{2c}, \tag{8}$$
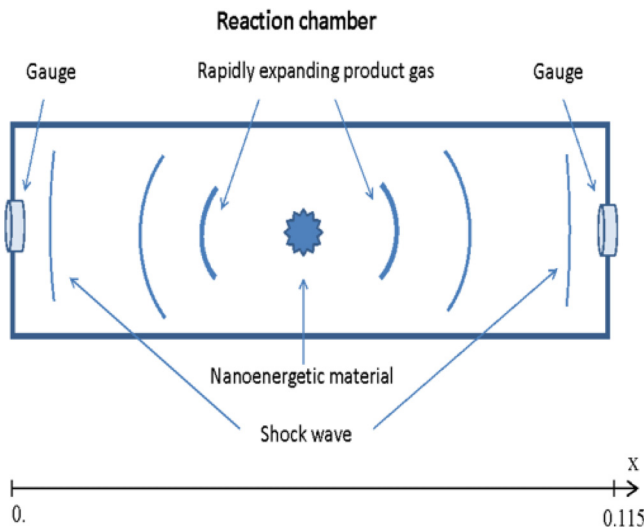
Reaction chamber

FIG. 1. Schematic diagram of a cylindrical reactor, closed at both ends. Explosion occurs in the middle of a cylindrical reactor. Fluid motion is uniform in a circular cross-section of the reactor.

where s is the speed of sound in the material behind the shock wave, and c is the viscous parameter in (2). A self-similar solution estimate as in Ref. 15 yields

$$s \sim \frac{2}{3} \frac{\sqrt{2\gamma(\gamma-1)\beta^3 h_e}}{\gamma+1}, \qquad (9)$$

for the material speed of sound right at the end of the reaction. The coefficient β depends on γ and was computed in Ref. 15, $\beta \approx 1.49$ for $\gamma = \frac{5}{3}$. This gives $s \sim 1000$ m/s for the Al/Bi$_2$O$_3$ reaction, giving an apriori estimate of linear stability condition, $\Delta t \leq 6.5 \times 10^{-4} [\text{s/m}] \frac{\Delta x}{c}$.

III. NUMERICAL SIMULATION: DETAILS AND RESULTS

It was recently shown that among common thermite nano-energetic materials, the reactions Bi$_2$O$_3$ + 2Al = Al$_2$O$_3$ + 2Bi and 3I$_2$O$_5$ + 10Al = 5Al$_2$O$_3$ + 6I generated the highest pressure discharge. A possible explanation for the high pressure rise during the combustion of Al/Bi$_2$O$_3$ and Al/I$_2$O$_5$ nanosystems is that the reaction product (bismuth or iodine) boils at a
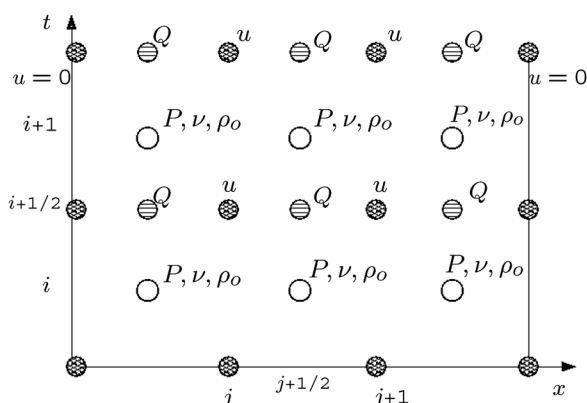

FIG. 2. Finite difference scheme.

temperature of 1560 and 184 °C, respectively, that is, lower than the maximum reaction temperature 2000 °C. This causes bismuth or iodine evaporation and increases the released gas pressure.

We have studied numerically a reaction which releases 1 kJ of energy (corresponding to about 0.5 g of Al/Bi$_2$O$_3$ mixture) in the reactor of volume $V = 0.342$ l. Reaction starts initially in a thin cross section of a cylinder, giving us a one-dimensional set-up. Following the experimental set-up, the reactor length L was established as 0.115 m. Ten thousand sample points were established equally along the length of the reactor for a finite difference approximation, $n_x = 10\,000$, $\Delta x = \frac{L}{n_x}$. Initially, there was a difficulty when the reaction was very close to a wall. To counter this problem, we took $c \sim 40$, and started the reaction in the middle of the reactor. With $c = 40$, the linear stability condition given in (8) with s estimated by the maximal speed using the numerical data, yields $\Delta t \leq 7.5 \times 10^{-11}$ s. In the actual computation we report, $\Delta t \leq 7 \times 10^{-13}$ s. The time of arrival of the shock wave to the wall can be estimated from the self-similar solution to be $t_* = 2.0 \times 10^{-5}$ s (2.6×10^{-5} s using numerics). Based on the linear stability condition, at least 260 000 time steps are required for a shock wave to reach the wall (36×10^6 in the actual computation). Either one of those iteration numbers is too high for the MATLAB/Mathematica software, so the coding was done in C.

To model the chemical reaction itself, a reaction region containing 200 mesh points was dedicated on the x axes to represent the region initially occupied by the solid energetic material, with a further 100 mesh points on the left and right end to turn on higher density using a smooth characteristic function. Initial density distribution of solid material was taken to be Gaussian (with the mean at the center of the reaction region and the standard deviation equal to the reaction region half-width) multiplied by a smooth characteristic function of the reaction region. This provided an initial density distribution smooth enough to enable numerical modeling of the early stages of the reaction. The "solid" region we obtained by this method is wider than it is in reality, with an average density in the initial "solid" region of 64 kg/m^3. With a fixed mesh, we will have too few mesh points if we try to start with a narrower region with solid-like densities. Since after the highly energetic reaction started, the material quickly expands out of the initial region, initial density does not have much effect on the subsequent fluid dynamics.

In Figure 3, the results are presented for the case when the reaction time is $\tau = 7 \times 10^{-8}$ s, which is consistent with a modeling results on rapid oxidation of nano-sized aluminum particle.[11] This short of a reaction time is the case for a "quick" reaction: after the reaction has ended, the high pressure region is not much wider than the narrow region initially occupied by the solid reagents. Subsequent fluid dynamics, illustrated in Figure 3, is consistent with a strong shock wave traveling out of the reaction region, hitting the reactor wall, reflecting back and making several further reflections. The results are presented in Eulerean coordinates X, which can be found once the solution in Lagrangian coordinates x is known, by integrating $\frac{\partial X}{\partial x} = \rho_o(x)\nu(x,t)$, $X(0) = 0$.

Computation provides the pressure at the center of the reaction just after the reaction was complete with a pressure of 1.3×10^8 Pa. That quantity is sensible and is consistent
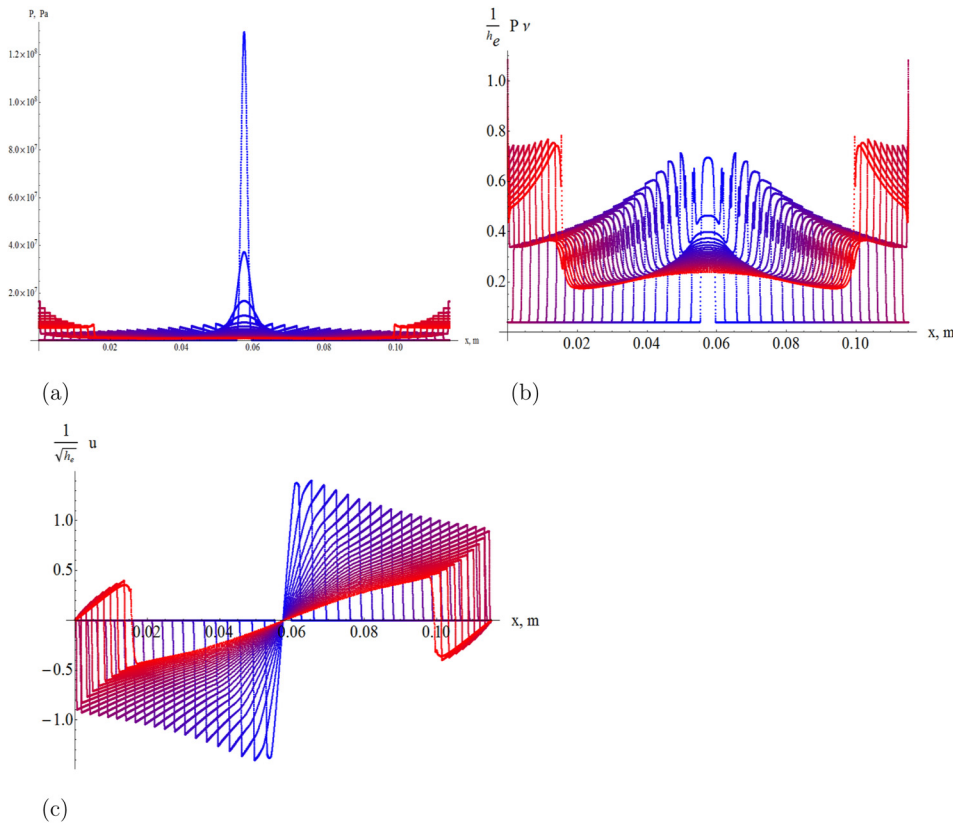
(a)

(b)

(c)

FIG. 3. Numerical modeling of an explosion of 0.5 g of Al/Bi$_2$O$_3$ mixture, starting in the middle cross-section of a closed cylindrical reactor of volume $V = 0.342$ 1 and length $L = 0.115$ m. Successive (a) pressure P (Pa), (b) dimensionless $\frac{1}{h_e} P\nu$, (c) dimensionless velocity $\frac{1}{\sqrt{h_e}} u$, as a function of Eulerean coordinate X along the cylinder axes, are shown in time steps of 1.3×10^{-6} s. Here P is pressure, ν is specific volume per unit mass, u is velocity, $h_e = 2.12$ MJ/kg is the reaction energy per unit mass. The reaction time is 7.0×10^{-8} s.
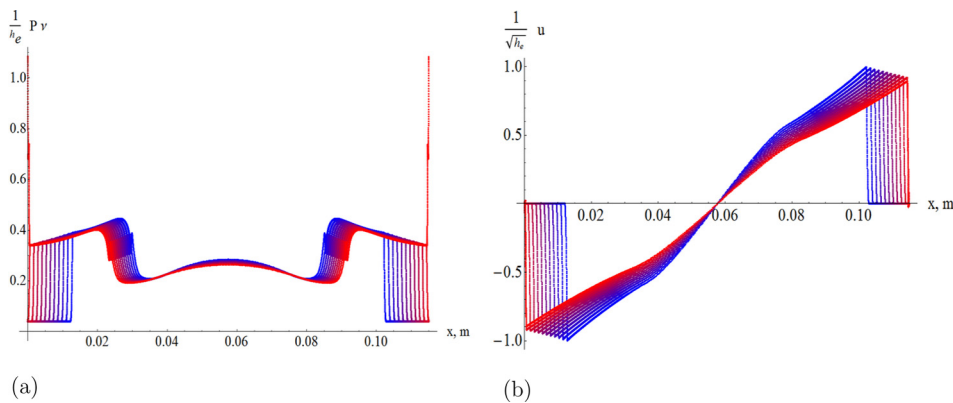

(a)

(b)

FIG. 4. Successive (a) dimensionless pressure $\frac{\nu_w}{h_e} P$ (b) dimensionless velocity $\frac{1}{\sqrt{h_e}} u$, as a function of Eulerean coordinate X along the cylinder axes, are shown at times up to the first impact with the base of a closed cylindrical reactor, in time steps of 6.3×10^{-7} s. Here P is pressure, $\nu_w = 0.14$, $\frac{m^3}{kg}$ is a typical specific volume at a time of the first impact with the base, u is velocity, h_e reaction energy per unit mass.

with an estimate based on the approximate conservation of the internal energy per unit mass during a quick reaction, ignoring expansion and work due to the pressure. Initial densities are lower than the solid densities. We anticipate that starting with higher density will yield higher pressures at the reaction center. Top velocities in our numerical computation were achieved right after the reaction ended and were about 2000 m/s, which is a bit higher than an estimate of 1700 m/s made on the basis of a self-similar solution.

Pressure, density, and velocity prior to the first impact with the wall are illustrated in Figure 4. Time dependence of pressure at the closed wall, at the base of cylindrical reactor, is shown in Figure 5.

The numerical results yield pressure on approach to the reactor wall of 3.16×10^6 Pa, increasing to 1.7×10^7 Pa on impact with the closed wall. Pressure on impact with the
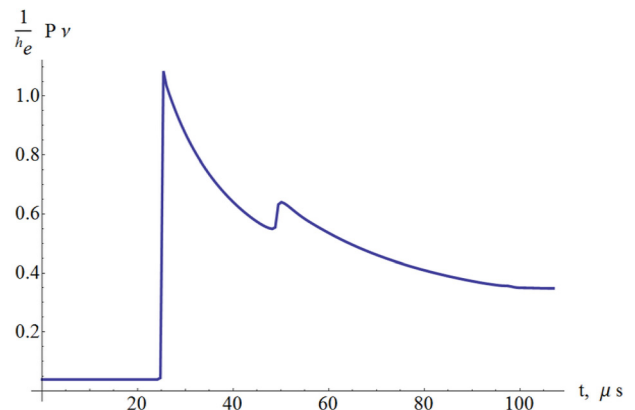

FIG. 5. Time dependence of the dimensionless $\frac{1}{h_e} P\nu$ at the base of a closed cylindrical reactor. Here P, ν is pressure and specific volume per unit mass at the reactor base, $h_e = 2.12$ MJ/kg is the reaction energy per unit mass.

closed wall is in good match with the experimental data presented in Refs. 12 and 16.

We note that in this paper, it was assumed that the reaction in the fuel region occurs very quickly, much faster than any other time scale present in the problem. Since the model is focused on modeling pressure wave in the reactor bulk, we did not model the finite flame velocity in the tiny fuel region. Finite flame velocity may be important in different experimental set-ups such as Parimi et Yetter.[20,21] We believe that supplementing fluid dynamics methods used in our paper with detailed models of a particle oxidation mechanism in the fuel region will help to explain the finite flame velocity experimental values.

IV. CONCLUSIONS

Direct numerical modeling results have been shown to be consistent with the experimental evidence and estimates based on the self-similar solution. Artificial viscosity provides sufficient smoothing of shock wave discontinuity for the numerical work to continue. The direct numerical method is more computationally demanding, and is more flexible than self-similar solutions, in particular it allows study of the early stages of the reaction (while the self-similar solution is singular). This allows the investigation of "slower" reactions, which may produce weaker shocks or no shocks at all (while the self-similar solution does not allow for a reaction time parameter). Moreover, the direct numerical method allows the flexibility to model reflections of the shock waves from the reactor walls. Numerical results indicate that at the center of explosion, pressure depends on the initial density of a material, and is roughly proportional to the initial density, and on reaction time. If shock wave runs away significantly from the center during the reaction time period, the pressure generation at the reaction center is lower. In the range of parameters explored, corresponding to sufficiently quick reactions, it appears that far away from the reaction center, the peak pressure is not very sensitive to the initial density and reaction time, provided that all the material reacts well before the shock wave arrives to the end of reactor (otherwise the peak pressure should be lower). It may be possible to extend the indicated numerical work to 3 dimensions such as to investigate numerically a reaction in non-symmetric domains, far from a cylindrical or spherical geometry. In the future, it will be interesting to perform these computations on a supercomputer, to understand effects of shock wave propagation in complex geometries in three spacial dimensions.

ACKNOWLEDGMENTS

[1]D. D. Dlott, "Thinking big (and small) about energetic materials," Mater. Sci. Technol **22**(4), 463 (2006).

[2]A. Prakash, A. V. McCormick, and M. R. Zachariah, "Synthesis and reactivity of a super-reactive metastable intermolecular composite formulation of Al/KMnO$_4$," Adv. Mater. **17**(7), 900 (2005).

[3]J. A. Puszynski, C. J. Bulian, and J. J. Swiatkiewicz, "Processing and ignition characteristics of aluminum-bismuth trioxide nanothermite system," J. Propul. Power **23**, 698 (2007).

[4]V. E. Sanders, B. W. Asay, T. J. Foley, B. C. Tappan, A. N. Pacheco, and S. F. Son, "Reaction propagation of four nanoscale energetic composites (Al-MoO$_3$, Al-WO$_3$, Al-CuO, and Bi$_2$O$_3$)," J. Propul. Power **23**(4), 707–714 (2007).

[5]G. Jian, S. Chowdhury, K. Sullivan, and M. R. Zachariah, "Nanothermite reactions: Is gas phase oxygen generation from the oxygen carrier an essential prerequisite to ignition," Combust. Flame **160**, 432–437 (2013).

[6]R. R. Nellums, B. C. Terry, B. C. Tappan, S. F. Son, and L. J. Groven, "Effect of solids loading on resonant mixed Al-Bi$_2$O$_3$ nanothermite powders, propellants, explosives," Pyrotechnics **38**(5), 605–610 (2013).

[7]A. R. Poda, R. D. Moser, M. F. Cuddy, Z. Doorenbos, B. J. Lafferty, C. A. Weiss, Jr., A. Harmon, M. A. Chappell, and J. A. Steevens, "Nano-aluminum thermite formulations: characterizing the fate properties of a nano-technology during use," Nanomater. Mol. Nanotechnol. **2**(1), 1000105 (2013).

[8]E. L. Dreizin, "Metal-based reactive nanomaterials," Prog. Energy Combust. Sci. **35**, 141–167 (2009).

[9]A. Ermoline and E. L. Dreizin, "Equations for the Cabrera-Mott kinetics of oxidation for spherical nanoparticles," Chem. Phys. Lett. **505**, 47–50 (2011).

[10]S. Mohan, A. Ermoline, and E. L. Dreizin, "Pyrophoricity of nano-sized aluminum particles," J. Nanopart. Res. **14**, 723 (2012).

[11]K. S. Martirosyan and M. Zyskin, "Reactive self-heating model of aluminum spherical nanoparticles," Appl. Phys. Lett. **102**, 053112 (2013).

[12]K. S. Martirosyan, L. Wang, A. Vicent, and D. Luss, Nanotechnology **20**, 405609 (2009).

[13]K. S. Martirosyan, L. Wang, A. Vicent, and D. Luss, Prop., Explos., Pyrotech **34**, 532 (2009).

[14]K. S. Martirosyan, L. Wang, and D. Luss, Chem. Phys. Lett. **483**, 107 (2009).

[15]K. Martirosyan, M. Zyskin, C. M. Jenkins, and Y. Horie, "Modeling and simulation of pressure waves generated by nano-thermite reactions," J. Appl. Phys **112**, 094319 (2012).

[16]K. S. Martirosyan, "Nanoenergetic gas generators, principles and applications," J. Mater. Chem. **21**, 9400–9405 (2011).

[17]Ya. B. Zel'dovich and Yu. P. Raizer, *Physics of Shock Waves and High-Temperature Hydrodynamic Phenomena* (Dover Publications, 2002).

[18]P. Lax, *Hyperbolic Systems of Conservation Laws and the Mathematical Theory of Shock Waves* (SIAM, 1973).

[19]J. VonNeumann and R. D. Richtmyer, "A method for the numerical calculation of hydrodynamic shocks," J. Appl. Phys. **21**, 232 (1950).

[20]V. S. Parimi, S. A. Tadigadapa, and R. A. Yetter, "Control of nanoenergetics through organized microstructures," J. Micromech. Microeng. **22**, 055011 (2012).

[21]J. Gesner, M. L. Pantoya, and V. I. Levitas, "Effect of oxide shell growth on nano-aluminum thermite propagation rates," Combust. Flame **159**, 3448–3453 (2012).